

# Solar-Powered/Fuel-Assisted Rankine-Cycle Power and Cooling-System: Simulation Method and Seasonal Performance

N. Lior  
K. Koai

Department of Mechanical Engineering  
and Applied Mechanics,  
University of Pennsylvania,  
Philadelphia, Pa 19104

*The subject of this analysis is a solar cooling system based on a novel hybrid steam Rankine cycle. Steam is generated by the use of solar energy collected at about 100°C, and it is then superheated to about 600°C in a fossil-fuel-fired superheater. The addition of about 20–26 percent of fuel doubles the power cycle's efficiency as compared to organic Rankine cycles operating at similar collector temperatures. A comprehensive computer program was developed to analyze the operation and performance of the entire power/cooling system. Transient simulation was performed on an hourly basis over a cooling season in two representative climatic regions (Washington, D.C. and Phoenix, Ariz.). One of the conclusions is that the seasonal system COP is 0.82 for the design configuration and that the use of water-cooled condensers and flat-plate collectors of higher efficiency increases this value to 1.35.*

## 1 Introduction

As compared to most of the other Rankine-cycle concepts for generating power from low-temperature (<150°C) solar energy sources, which are characterized by using organic working fluids and powered by solar energy alone (see reviews in [1–5]), the concept described here uses steam in a hybrid solar/fossil-powered cycle. The principle of this concept is the elevation of the top cycle temperature by superheating the steam to improve cycle efficiency, and use of energy from two different temperature levels to provide better thermodynamic matching with the energy sinks in the cycle. Since the boiling of the water is accomplished at relatively low temperatures (around 100°C), about 80 percent of the heat can be supplied by solar collectors at this relatively low temperature, and the remaining 20 percent needed for superheating (up to about 600°C) can be supplied by fossil fuel (see analyses in [1, 5–7]). These analyses have shown that at the same time the efficiency of the Rankine cycle is essentially doubled when compared to that of organic fluid Rankine cycles that operate at similar solar collector temperatures, from about 9 to about 18 percent. Since the solar collectors account for a major fraction of the total system's cost (typically more than a half), of most significance is the fact that this hybrid cycle, named SSPRE (Solar Steam Powered Rankine Engine, pronounced 'espre'), was found in the aforementioned studies to require only about half the collector area as compared to cycles using organic fluids, and to operate at a lower collector temperature at that. At present collector and fuel prices, the SSPRE concept has a major economic advantage. Rising fuel costs and possibly declining collectors costs may change this situation, but at

such time solar concentrators are expected to become sufficiently economical so that they may replace fossil-fuel superheating, for an all-solar operation. Here again, the principle of matching energy sources and sinks of similar temperature allows the use of low-temperature, low-cost collectors to supply the major portion of the energy (latent heat), and the use of a small quantity of high-temperature higher-cost concentrators to supply the superheat.

The SSPRE system with application to solar cooling has been under analytical and hardware development at the University of Pennsylvania for a number of years, (testing is due to start soon) and its flow diagram is shown in Fig. 1. Heat recovery within the cycle is obtained by a regenerator

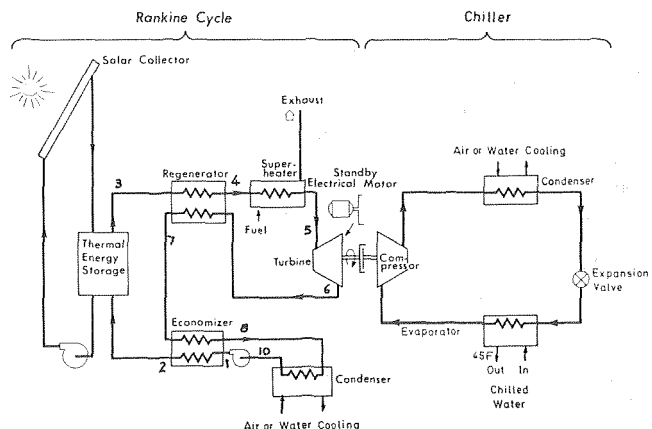


Fig. 1 The solar-powered/fuel-superheated steam Rankine cycle (SSPRE) driving a vapor-compression chiller

Contributed by the Solar Energy Division for publication in the JOURNAL OF SOLAR ENERGY ENGINEERING. Manuscript received by the Solar Energy Division June 25, 1982.

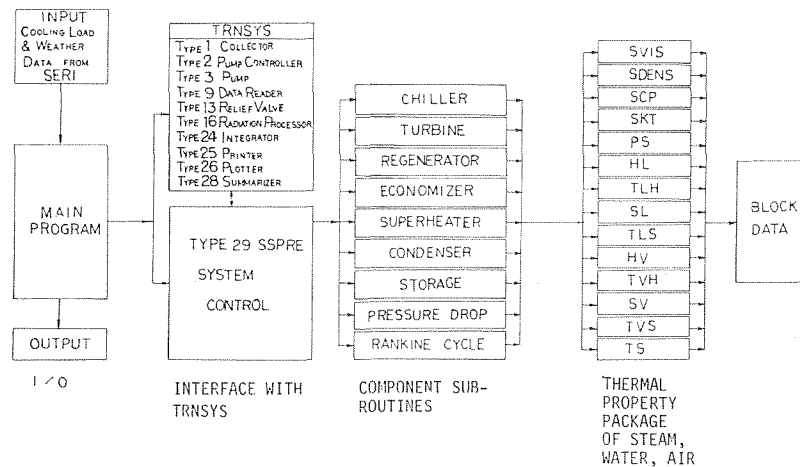


Fig. 2 Structure of the SSPRE program

and economizer. At present, its power output of 30 hp (at design) is intended to drive a commercial open-compressor, 25-ton (nominal) vapor compression chiller. Since low-horsepower commercial steam turbines operate at low efficiency, typically below 50 percent, a novel 30-hp, radial-flow, 10-stage turbine with 25-cm-dia counterrotating rotors, which utilizes reaction blading, was designed and built [8].

This type of hybrid cycle is not confined to solar energy or solar cooling, but retains its advantages when used with any low-temperature energy sources, such as waste heat or geothermal heat (see [9-12]), and can be designed to produce power at rates up to those of conventional utility power plants.

A comprehensive computer program was developed for transient analysis of the operation and performance of the entire power/cooling system and simulations were performed on an hourly basis for a 4-month cooling season in two representative climatic regions, for a number of system configurations. The computer program and the results of the analysis are described below.

## 2 System Modeling

**2.1 The General Method.** Each system component was described by a separate subroutine to compute its performance from basic principles, and special attention was given to the parasitic losses, including pumps, fans, and

pressure drops in the piping and heat exchangers, and to the description of off-design performance of the components. The needed thermophysical and transport properties of the fluids used here were also described as a function of the independent parameters, in separate subroutines. The input to the program consists of the system's configurational and operational parameters, such as geometry and materials of components, temperature bounds, and hourly cooling load and weather and insolation data. The output consists of the values of state parameters of the system, the status of all components (say off or on), and the various performance criteria (such as efficiencies and coefficients of performance). These values are obtained for each time increment, and also integrated for a desired period. As constructed, the program allows the examination of the system's performance for practically arbitrary configurations, loads, and climatic regions.

New subroutines were developed to calculate the performance of all Rankine cycle components, the thermal storage, the chiller, the control strategy, and the fluid properties and were combined into program "SSPRE." The program TRNSYS [13] was used to determine the performance of the solar loop (collectors, pump, controls, etc.) as well as for some utility functions, and was linked to "SSPRE." The structure of the overall program is shown in Fig. 2.

## Nomenclature

$A_1$  = surface area of thermal storage tank  
 $A_x$  = free surface area of water in flash-tank storage  
 $B$  = coefficient of evaporation rate, from [21]  
 FUEL = fuel mass flow rate to superheater, (kg/hr)  
 $h$  = enthalpy  
 HFUEL = total heat value of fuel supplied to superheater, (FUEL)•(Lower Heating Value), (kJ/hr)  
 HLOAD = cooling load, (kJ/hr)  
 HPFAN = fan power for air-cooled condenser in Rankine cycle, (hp)  
 $I$  = insolation, kJ/hr•m<sup>2</sup>  
 MLOAD = total cooling load handled by the back-up electric motor, (kJ)  
 $\dot{m}_s$  = steam flow rate in Rankine cycle, kg/hr  
 $N$  = number of operating hours of the back-up electric motor  
 $P$  = pressure  
 POWER = turbine power output, (hp)  
 PVMAX = power output from ideal turbine with 100 percent efficiency, (hp)

PWMOT = back-up electric motor power, (hp)  
 QCON = heat transfer in condenser,  $\dot{m}_s(h_8 - h_{10})$ , (kJ/hr)  
 QEC = heat transfer in economizer,  $\dot{m}_s(h_7 - h_8)$ , (kJ/hr)  
 QLOSS = heat loss through thermal storage tank insulation to ambient, (kJ/hr)  
 QOVER = total energy discarded by the relief valve, (kJ)  
 QREG = heat transfer in regenerator,  $\dot{m}_s(h_6 - h_7)$ , (kJ/hr)  
 QSUP = heat transferred to steam in superheater,  $\dot{m}_s(h_5 - h_4)$ , (kJ/hr)  
 RAD = solar radiation flux incident on the collector surface, kJ/m<sup>2</sup> hr  
 RLOAD = total cooling load handled by the Rankine engine, (kJ)  
 $t$  = time  
 $T$  = temperature  
 $T_{CIN}$  = temperature of water at inlet to collectors  
 $T_{CL}$  = temperature of water at outlet from collectors

The new subroutines are briefly described below. More detail is provided in [14]. Since the turbine, superheater, and regenerator have been described elsewhere [7, 8], their description would not be repeated here. All the subroutines were validated, both by a manual calculation and by comparing to manufacturers' data.

## 2.2 Component Modeling.

**2.2.1 The Rankine-Cycle Condenser.** An air-cooled, fin-tube condenser was modeled to include two sections in series: a desuperheating section occupying a fraction  $F_x$  of the total tube length, followed by a condensing section. The procedure is conventional, following [15, 16], to calculate the condenser effectiveness, total heat transfer rate, and condensation temperature and pressure, as a function of steam and air-mass flows and inlet conditions, and of the condenser's configuration.

The air-side heat transfer coefficients were obtained from [17]. Pure convection heat transfer coefficients for the internal steam flow in the desuperheater section are provided for both laminar and turbulent regimes, to allow proper calculation for any combination of independent variables. The internal condensation heat transfer coefficient is calculated following [18].

The solution is iterative: (i) the air-side heat transfer coefficients are calculated for the airflow, air temperature and pressure, and condenser geometry; (ii) the weighted fin efficiency is then obtained; (iii) the steam-side heat transfer coefficient is calculated for the desuperheater section; (iv) the condensing temperature, and after assuming  $F_x$  also the overall heat transfer coefficients, effectiveness, and heat transfer rates, are calculated for both the desuperheating and condensing section; (v) the quality of the fluid at desuperheater exit is calculated, and if it is higher than a given value (2.5 percent used here), a corrected value of  $F_x$  is assumed and steps (iv) and (v) repeated till convergence.

**2.2.2 The Economizer.** After transferring some of its heat in the regenerator and before it comes to the condenser, the turbine exhaust steam transfers more heat to preheat the condensate. The latter process takes place in the economizer, which is a shell and tube (multipass) heat exchanger, with longitudinal fins on the tubes' exterior where the steam flows. Both here and in the regenerator, the effectiveness, total heat transfer rate, outlet temperatures, and internal pressure drops

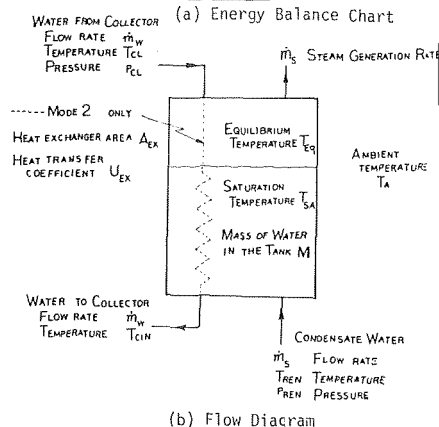
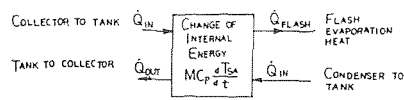


Fig. 3 Thermal energy storage tank schematic

of both streams are calculated as a function of the steam and water mass flows and inlet states, and of the heat exchanger's configuration. The calculation is conventional [15, 16], but somewhat more complex than in the regenerator, because of the different phase of each stream and of the existence of fins.

**2.2.3 Thermal Storage.** The thermal storage proposed for the SSPRE cycle consists of water heated by circulation through the solar collectors (Fig. 1). The hot water in the storage tank is allowed to flash into steam by reducing the pressure there. The flashed steam drives the turbine and recirculates into the tank after it is condensed. The method allows the use of the same fluid, water, for the storage and the power cycle, and minimizes heat exchanger penalties associated with most other storage methods. It has been widely used in Europe in the past (mostly in a process plants and steam locomotives) [19], and some renewed interest was expressed in the last decade (see [20]).

The analysis was developed for two alternative methods of supplying solar heat to the tank: a direct one, where the tank-water is circulated through the collectors (Mode 1), and one which separates the tank's water from that circulating through the collectors by a heat exchanger (Mode 2). The

## Nomenclature (cont.)

TFUEL, THFUEL, THLOAD, THPFAN, TQCON, TQEC, TQLOSS, TQOVER, TQREG, TQSOP, TPOWER, TPWMAX, TPWMOT, TRAD, TYAUX, TYCHIL, TYMOT, TYPOWER, TYPUMP, TYSOL, TYTANK = The first letter T in all these variables indicates the total integrated value, over the time period considered, of the parameter defined by the remaining letters following the T.

TOTAL = total power applied to chiller's compressor = TPOWER + TPWMOT

$U$  = overall heat transfer coefficient

YAUX = Rankine cycle parasitic energy (kJ/hr), containing the energy consumption by two pumps (one in collector loop, the other in Rankine loop) and two fans (one in superheater, the other in condenser).

YCHIL = energy consumption by the condenser fan in the chiller, (kJ/hr)

YMOT = back-up electric motor power, (kJ/kr)

YPUMP = power demand by Rankine cycle pump, (kJ/hr)

YSOL = net solar energy gain by the water in the collectors, (kJ/hr)

YTANK = energy supplied to cycle from storage tank,  $m_s(h_3 - h_2)$ , (kJ/hr)

## Greek

$\Delta P$  = pressure drop

$\epsilon_c$  = condenser effectiveness

$\epsilon_e$  = economizer effectiveness

$\epsilon_r$  = regenerator effectiveness

$\eta_e$  = electric energy generation and transmission efficiency

$\eta_{\text{motor}}$  = efficiency of electric motor

## Subscripts

Eq = final equilibrium vapor pressure in thermal storage flash tank

REN = return of water from power cycle to thermal storage tank

SA = saturation conditions in thermal storage tank

1-10 = refer to cycle states as described in Fig. 1

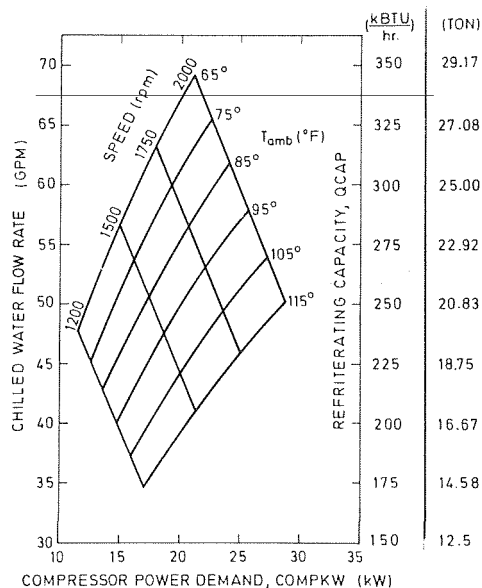


Fig. 4 Chiller performance. Chilled water in: 54°F (12.2°C); chilled water out: 44°F (6.7°C); cylinder loading fraction = 100 percent.

calculation provides the transient steam generation rate  $\dot{m}_s$ , and water and steam temperatures and pressures ( $T_{SA}$ ,  $P_{SA}$ ) as a function of tank and heat exchanger geometry, rate of heat input from the solar collectors (collector loop mass flow rate  $\dot{m}_w$ , inlet and outlet temperatures  $T_{REN}$ ,  $T_{CL}$ ,  $T_{CIN}$ ), and heat loss rate from the tank wall to the ambient (at ambient temperature  $T_A$ ).

The basic configuration of this thermal storage system is shown in Fig. 3. The analysis uses in Mode 1 the transient heat balance equation

$$M \frac{dh_{SA}}{dt} = \dot{m}_w (h_{CL} - h_{SA}) - UA_1 (T_{SA} - T_A) + h_{fl} \quad (1)$$

The left-side term expresses the rate of heat storage in the tank that contains a mass of water  $M$ , and the terms on the right-hand side express the heat added from the collector loop, the heat loss through the tank's insulation, and the heat  $h_{fl}$  carried away with the evolving steam respectively.

$$h_{fl} = \dot{m}_s (h_{REN} - h_{SA}) \quad (2)$$

where, by using the correlation from [21], the mass flow rate of steam  $\dot{m}_s$  is

$$\dot{m}_s = BA_x T_{Eq}^{-0.6} (P_{SA} - P_{Eq}) \quad (3)$$

In Mode 2, the first term on the right-hand side of equation (1) is replaced by the term  $U_{EX} A_{EX} [(T_{CL} + T_{CIN})/2 - T_{SA}]$  where  $U_{EX}$  and  $A_{EX}$  are the overall heat transfer coefficient and area of the internal heat exchanger, respectively.

The first-order differential equation in either mode is solved by a modified-Euler method (first-order predictor-corrector algorithm), with the initial value given.

**2.2.4 Pressure Drop.** Pressure drops are calculated both in the heat exchangers and in the interconnecting pipes, as a function of the flow channel geometry and roughness, and fluid flow rate, temperature, and pressure. The conventional equations (see [22]) are used for laminar or turbulent flow. Additionally, it is possible to substitute a manufacturer's pressure drop versus flow rate relationship into subroutines which compute the pressure drops in heat exchangers. This is particularly useful for units with complex flow geometries.

**2.2.5 Pump and Fan Power.** Based on the predetermined pressure drop, fluid flow rate, and device efficiency, the power demand of the pumps in the Rankine cycle and the collector loop, of the combustion air blower in the

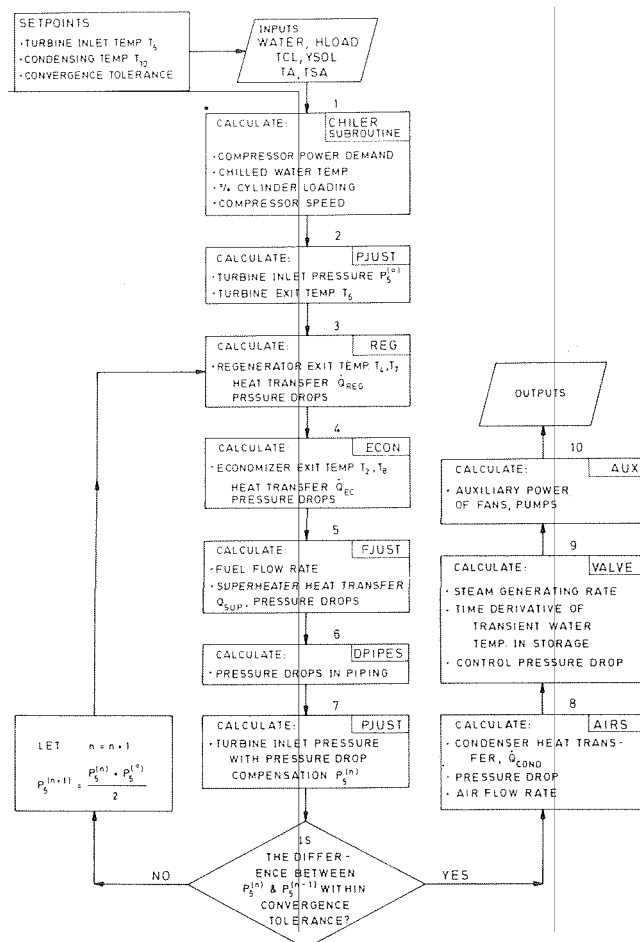


Fig. 5 Logic flow diagram of the SSPRE system program

superheater, and of the Rankine cycle condenser fans is computed.

**2.2.6 Chiller.** Since an air-cooled commercial chiller was planned for use with the SSPRE cycle, the manufacturer's data [23] were converted to a subroutine which computes its performance (refrigerating capacity QCAP, chilled water flow rate, and compressor power demand COMPKW) as a function of the ambient temperature  $T_{amb}$ , compressor rotation speed, cylinder loading fraction (%), and chilled water inlet/outlet temperatures. The chiller's capacity may be controlled by varying the compressor's speed (1200–2000 rpm; 1750 rpm nominal) and by unloading cylinders (up to three of the five cylinders may be unloaded). A typical performance chart for 100 percent loading is shown in Fig. 4.

**2.2.7 The Control Strategy.** Knowing the hourly cooling load and ambient conditions (input), the chiller subroutine is called to determine the compressor-speed/unloading combination that demands the least amount of power from the SSPRE cycle. Keeping the inlet temperature to the turbine constant at the maximum of 600°C, the turbine subroutine is called to determine the required steam inlet pressure and flow rate to provide the desired power. This could be obtained in practice by modulating the steam valve at the exit from the storage flash-tank. Work is being done at present to extend this scheme to seek the optimal (energy or economic) turbine inlet pressure-temperature combination which supplies the desired shaft power.

Once the steam flow rate and conditions are thus known, the superheater subroutine is called to determine the fuel flow rate, and the condenser subroutine is called to determine the cooling fan power needed to condense the steam. Whenever

the Rankine cycle/storage system is unable to supply the power needed by the chiller's compressor, or when resource energy saving cannot be attained, the back-up electric motor is turned on to drive the compressor, and steam flow to the turbine is stopped.

**2.3 Computation Logic.** The sequence of computation and its logic, based on the subroutines and control strategy described above, is displayed in Fig. 5. Energy balances are performed both on individual components and on the whole system, as an added measure to ensure that the results are correct.

**2.4 Major Performance Parameters.** Apart from computing the hourly and integrated values of the various energy inputs and outputs in the system, a number of energy fractions and performance criteria are determined, as described below.

Energy fractions<sup>1</sup>:

- Solar Energy:  $ZSOL = YSOL/SOTIN$  (4)

where SOTIN is the total resource energy used:

$$SOTIN = YSOL + HFUEL + E/\eta_e \quad (5)$$

and  $E$  is total electric energy used:

$$E = YAUX + YCHIL + YMOT \quad (6)$$

- Fuel energy:  $ZFUEL = HFUEL/SOTIN$  (7)

- Electric energy:  $ZE = \frac{E}{\eta_e}/SOTIN$  (8)

Further,  $ZE$  can be split into

- RC parasitic:  $ZAUX = \frac{YAUX}{\eta_e}/SOTIN$  (9)

- Chiller parasitic:  $ZCHIL = \frac{YCHIL}{\eta_e}/SOTIN$  (10)

- Backup motor:  $ZMOT = \frac{YMOT}{\eta_e}/SOTIN$  (11)

The percentile contribution of the Rankine engine:  
In terms of total cooling load<sup>2</sup>:

- $\%_0CL = \frac{\{\text{Total cooling load handled by the Rankine engine}\}}{\text{Total cooling load of the building}}$   
 $= \frac{RLOAD}{THLOAD}$  (12)

In terms of total power demand by the compressor:

- $\%_0RC = \frac{\text{Total power supplied by the turbine}}{\text{Total power demand by the compressor}}$   
 $= \frac{YPOWER}{YPOWER + YMOT}$  (13)

Efficiencies:

Collector:

- $\tilde{\eta}_{coll} = TYSOL/TRAD$  (14)

Thermal efficiency of the Rankine cycle

- $ZRANK = \frac{\text{Turbine work output}}{\text{Net energy gain in Rankine cycle}}$   
 $= \frac{TYPOWER}{TQSUP + TYTANK + TYPUMP}$

$$= \frac{\int \dot{m}_s (h_5 - h_6) dt}{\int \dot{m}_s [(h_5 - h_4) + (h_3 - h_2) + (h_1 - h_{10})] dt} \quad (15)$$

All subscripts of enthalpies refer to Figs. 1 and 6.

Overall Rankine cycle efficiency:

- $OZRANK = \frac{\text{Turbine work output}}{\{\text{Total energy input including parasitic energy}\}}$   
 $= \frac{TYPOWER}{TYTANK + THFUEL + TYAUX}$  (16)

Rankine cycle resource efficiency:

- $OZRANR = \frac{TYPOWER}{TYTANK + THFUEL + TYAUX/\eta_e}$  (17)

Coefficients of Performance (several definitions are used, because of the mix of energy inputs):

Chiller COP excluding parasitic power to fan:

- $COPNF = \frac{\text{Total cooling load}}{\{\text{Total power demand by the compressor}\}}$   
 $= \frac{THLOAD}{TYPOWER + TYMOT}$  (18)

Chiller COP, including parasitic power to fan:

- $COP = \frac{\text{Total cooling load}}{\{\text{Total power demand by the compressor}\} + \{\text{and the parasitic power of the chiller}\}}$   
 $= \frac{THLOAD}{TYPOWER + TYMOT + TYCHIL}$  (19)

Overall system COP based on total energy input, including all parasitic energy:

- $OCOPP = \frac{\text{Total cooling load}}{\text{Total energy input}}$   
 $= \frac{THLOAD}{TYSOL + THFUEL + TYAUX + TYCHIL + TYMOT}$  (20)

Overall system COP based on resource energy input:

- $OCOPP = \frac{\text{Total cooling load (THLOAD)}}{\text{Total resource energy input (SOTIN)}}$   
 $= \frac{THLOAD}{TYSOL + THFUEL + (TYAUX + TYCHIL + TYMOT)/\eta_e}$  (21)

Overall system COP based on total energy energy conversion excluding all parasitic energy:

- $OCOPS = \frac{\text{Total cooling load}}{\text{Total net energy conversion}}$   
 $= \frac{THLOAD}{TYTANK + TQSUP + TYPUMP + TYMOT}$  (22)

Overall system COP based on total thermal energy input:

- $OCOPT = \frac{\text{Cooling load handled by Rankine engine}}{\text{Total thermal energy input}}$   
 $= \frac{RLOAD}{TYTANK + TQSUP}$  (23)

The percentile resource energy saving:

Here total energy saving is evaluated as compared with the same chiller driven entirely by an electric motor. Normalized by the total energy consumption of the electric chiller system, the percentile resource energy saving is computed as follows:

<sup>1</sup>Terms undefined in the text are defined in the Nomenclature.

<sup>2</sup>The prefix T indicates the total integrated value, over the specified period, of the parameter HLOAD. This convention is used throughout the paper.

$$\bullet \text{ ZSAV} = (100\%) \frac{\left\{ \frac{\text{TYPOWER} + \text{TYMOT} + \text{TYCHIL}}{0.3\eta} \right\} - \left\{ \frac{\text{TYMOT} + \text{TYCHIL} + \text{TYAUX}}{0.3\eta_{\text{motor}}} + \text{THFUEL} \right\}}{\left\{ \frac{\text{TYPOWER} + \text{TYMOT} + \text{TYCHIL}}{0.3\eta_{\text{motor}}} \right\}}$$

$$= (100\%) \frac{\{\text{TYPOWER} - \text{TYAUX} - 0.3\eta_{\text{motor}} \text{THFUEL}\}}{\text{TYPOWER} + \text{TYMOT} + \text{TYCHIL}} \quad (24)$$

The electric energy saving:

For an economic analysis, which compares the energy cost of an electrically driven chiller with that operated by the SSPRE system, only the electric energy saving (EES) needs to be evaluated against the fuel consumption in the superheater (THFUEL).

$$\begin{aligned} \bullet \text{ EES} &= \left[ \begin{array}{l} \text{Total electric energy} \\ \text{used by motor-driven} \\ \text{chiller system} \end{array} \right] \\ &\quad - \left[ \begin{array}{l} \text{Total electric energy} \\ \text{used by SSPRE} \\ \text{system} \end{array} \right] \\ &= \left\{ \frac{\text{TYPOWER} + \text{TYMOT} + \text{TYCHIL}}{\eta_{\text{motor}}} \right\} \\ &\quad - \left\{ \frac{\text{TYMOT} + \text{TYCHIL} + \text{TYAUX}}{\eta_{\text{motor}}} \right\} \\ &= \frac{\text{TYPOWER} - \text{TYAUX}}{\eta_{\text{motor}}} \quad (25) \end{aligned}$$

### 3 Results

**3.1 Conditions and Configuration for the Runs.** Hourly weather, insolation, and cooling load data for a small office building with a 25-ton nominal cooling load were obtained from a SERI tape [24] and runs were performed for a 4-month (May–August) cooling season for two different climatic regions. Washington D.C. was selected to represent a Northeastern city which has moderate sunshine (64 percent summer sunshine) and moderate cooling load (1080 annual cooling hrs). The Phoenix commercial load represents the high end for a Southwestern city, with the highest percentage of summer sunshine (84 percent) and the largest number of cooling hours (2750 annually).

The “base-case” system configuration consisted of 37 m<sup>3</sup> water for storage, a regenerator having a heat transfer area of 14.9 m<sup>2</sup>, an economizer with a finned area of 17.6 m<sup>2</sup>, and an air-cooled condenser with a finned area of 763 m<sup>2</sup> (31.8 m<sup>2</sup> for the tubes alone). 200 m<sup>2</sup> of solar collectors characterized by the equation<sup>3</sup>

$$\eta_{\text{coll}} = 0.391 - 4.579 \left( \frac{T_i - T_a}{I} \right) \quad (26)$$

where the slope is in (kJ/hr m<sup>2</sup> °C), were used. The collector has the following incidence angle modifier  $K_{\text{air}}$

Angle of incidence deg	$K_{\text{air}}$
0	1.000
15	1.070
30	1.130
45	1.104

The superheater is gas-fired and has a heat transfer area of

0.73 m<sup>2</sup> in a parallel-flow furnace section, and 4.23 m<sup>2</sup> in a counterflow convection section<sup>4</sup>.

The chiller was described in Section 2.2.6.

A relief-valve subroutine in TRNSYS was used to limit the temperature in the storage tank to a maximum of 130°C.

**3.2 Transient Performance.** To demonstrate a typical set of operating conditions, the temperatures, pressures, and pressure-drops for one of the runs are shown in Fig. 6. It is noteworthy that the pressure drops reduce the available steam pressure ratio across the turbine by 9.3 percent, and thus reduce the power output by a similar percentage. This effect was seldom, if ever, considered in past analyses but, as shown here, should not be ignored.

To attain basic understanding of the process, the transient energy interactions and temperatures were examined. Figure 7(a) shows the hourly values for a typical day in Washington, D.C., and Fig. 7(b) is for Phoenix, Arizona. The shown hourly cooling load and sum of energy flows from the fuel, the storage tank and the parasitic and backup electric energy, also allow the easy determination of the hourly or averaged overall system COP. Figure 7(b) shows that the backup motor was engaged between 13:00 and 15:00.

Figure 8(a,b) shows the variations of the temperature and total energy in the storage tank on a typical day. The decrease of stored thermal energy corresponds to the heat extraction from the storage during the system’s normal operation. In Fig. 8(b) it can be seen that the tank restores its temperature and total energy between 13:00 and 15:00, when the backup motor is in operation.

Figures 9(a,b) and 10(a,b) show the daily results for a typical week and reflect the fact that there is no cooling load in the office building on weekends, during which time the thermal storage is recharged by continuing collection of solar energy.

The seasonal energy inputs and load are shown, month by

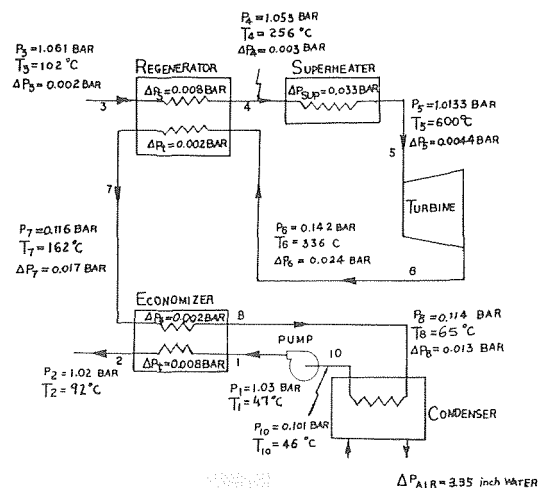
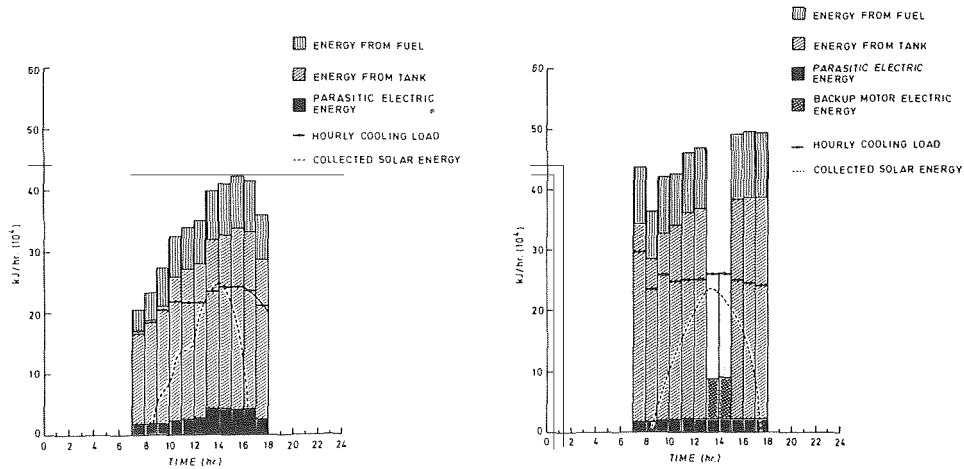


Fig. 6 Typical steam temperature, pressure, and pressure-drop (through the heat-exchangers and a total 3 m equivalent length of 2.5-in.-i.d. pipe)

<sup>3</sup>Sun Master DEC8A, all data according to [25]

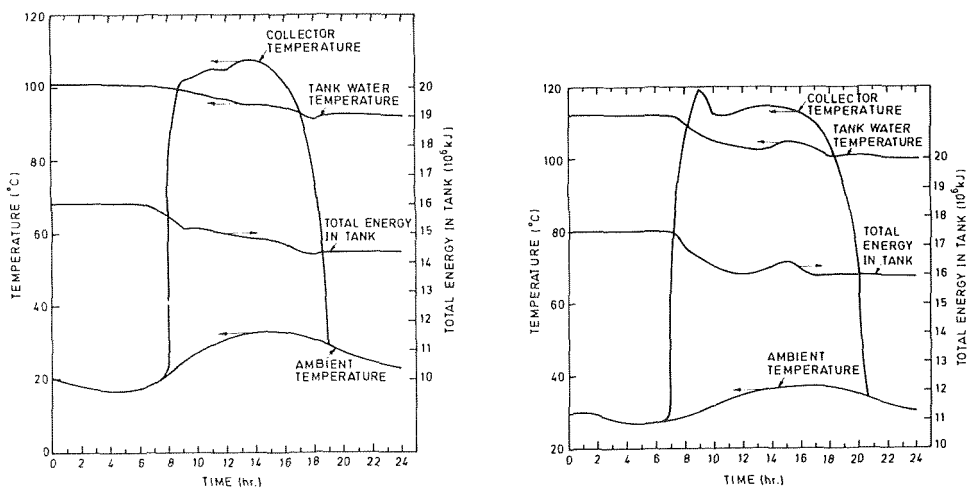
<sup>4</sup>A unit like this was built to the University of Pennsylvania specifications by Trane Thermal Co., Conshohocken, Pa.



a: Washington, DC, August 13

b: Phoenix, AZ, August 14

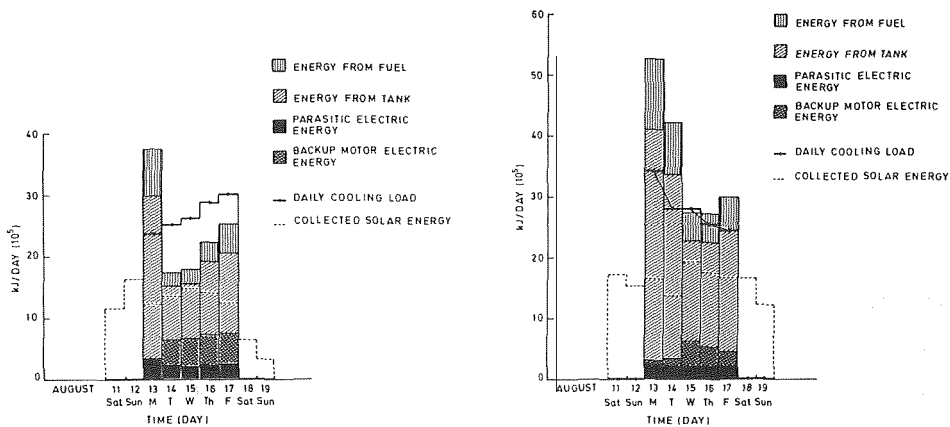
Fig. 7 Hourly energy map



a: Washington, DC, August 13

b: Phoenix, AZ, August 14

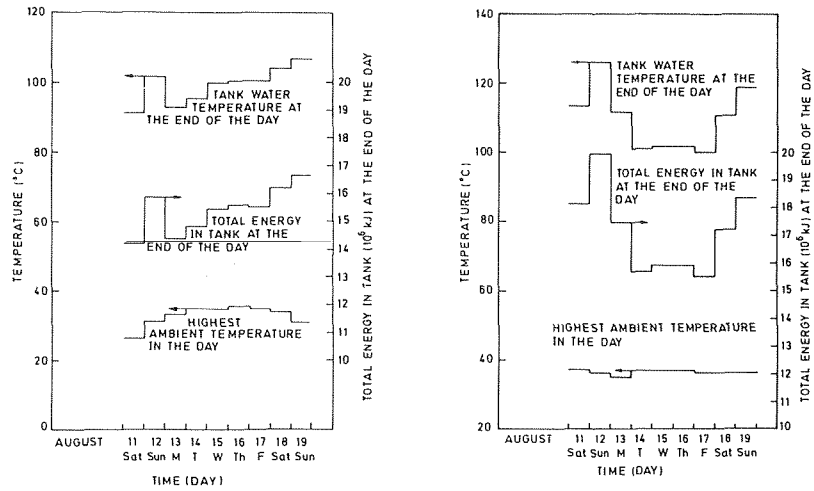
Fig. 8 Hourly variation of temperatures and of stored energy



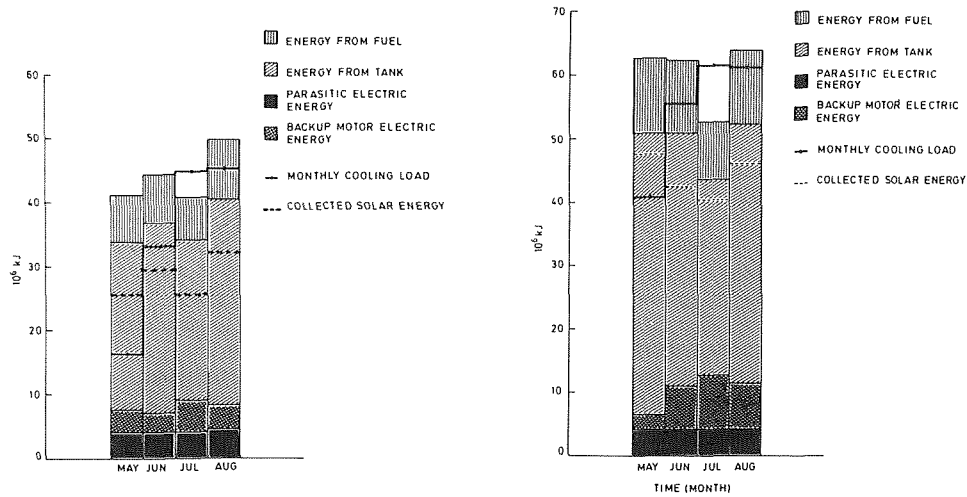
a: Washington, DC

b: Phoenix, Az

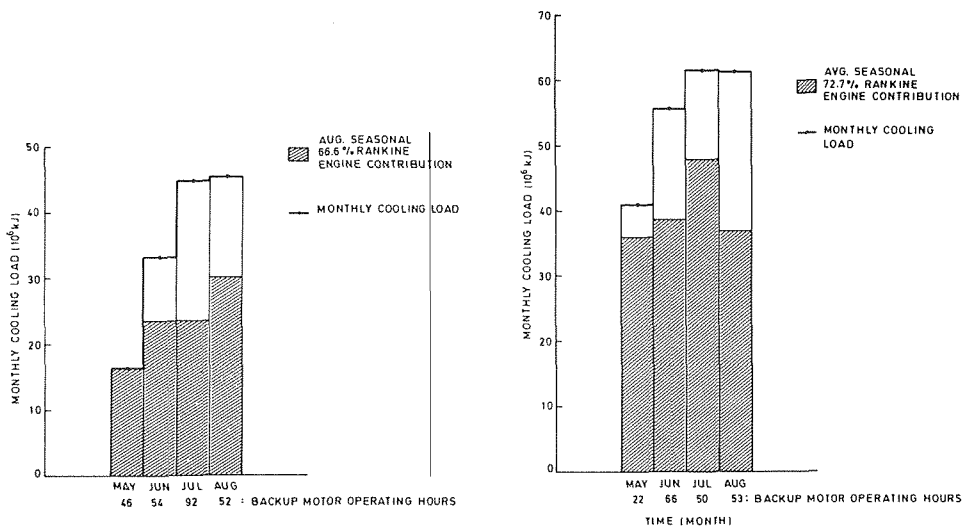
Fig. 9 Daily energy map over one week in August



a: Washington, DC  
 b: Phoenix, AZ  
**Fig. 10** Daily variation in storage tank temperature and energy at the end of the day, and in peak daily ambient temperature, for one week in August



a: Washington, DC  
 b: Phoenix, AZ  
**Fig. 11** Monthly energy map for a cooling season



a: Washington, DC  
 b: Phoenix, AZ  
**Fig. 12** Monthly cooling load satisfied by the SSPRE, for a cooling season

**Table 1 Detailed simulation results for the base-case SSPRE/cooling system for a four-month cooling season**

Parameter	Units	Washington, DC					Phoenix, AZ				
		May	June	July	August	Total	May	June	July	August	Total
TFUEL	kg	189.9	199.3	257.1	233.8	880.1	313.7	316.0	254.0	341.2	1224.9
THFUEL	10 <sup>6</sup> kJ	9.517	9.981	0.752	11.710	39.960	15.72	15.83	12.73	17.10	61.38
TYAUX	10 <sup>6</sup> kJ	0.781	0.631	0.635	1.004	3.051	0.562	0.617	0.589	0.724	2.492
TYCHIL	10 <sup>6</sup> kJ	3.437	3.762	3.762	3.762	14.720	3.728	3.762	3.728	3.762	14.980
THPFAN	hp-hr	224.9	160.4	159.6	301.8	846.7	31.90	77.75	89.32	120.80	319.77
TPOWER	hp-hr	2103	2180	1869	2479	8631	2956	2836	2222	3016	11030
TPWMOT	hp-hr	1321	1067	1890	1387	5665	797.1	2576	3375	2728	9476.1
TOTAL	hp-hr	3424	3247	3759	3866	14296	3753	5412	5597	5744	20506
TYPOWER	10 <sup>6</sup> kJ	5.648	5.855	5.020	6.658	23.180	7.939	7.616	5.967	8.100	29.620
TYMOT	10 <sup>6</sup> kJ	3.548	2.866	5.076	3.725	15.210	2.141	6.918	9.064	7.326	25.450
TYSOL	10 <sup>6</sup> kJ	25.95	29.72	25.71	31.17	112.55	47.89	42.57	40.36	46.20	177.02
TRAD	10 <sup>6</sup> kJ	102.74	119.60	100.00	111.30	433.60	161.7	148.3	144.0	158.2	612.2
THLOAD	10 <sup>6</sup> kJ	16.56	33.38	45.03	45.52	140.50	40.99	55.69	61.46	61.32	219.50
RLOAD	10 <sup>6</sup> kJ	13.24	23.58	23.65	33.02	93.49	36.03	38.79	47.95	36.89	159.66
MLOAD	10 <sup>6</sup> kJ	3.325	9.797	21.380	12.500	47.000	4.96	16.90	13.51	24.43	59.80
TPWMAX	hp-hr	2860	2996	2581	3423	11860	4053	3878	3032	4114	15077
TYTANK	10 <sup>6</sup> kJ	26.19	29.02	24.88	32.83	112.90	44.12	39.84	30.80	41.11	155.87
TQSUP	10 <sup>6</sup> kJ	7.402	7.835	6.812	9.066	31.120	11.83	11.43	9.03	12.14	44.70
TQREG	10 <sup>6</sup> kJ	4.500	5.460	4.592	5.971	20.520	8.576	6.856	5.070	6.650	27.152
TQEC	10 <sup>6</sup> kJ	1.714	1.907	1.689	2.250	7.560	3.264	3.088	2.430	3.221	12.000
TQCON	10 <sup>6</sup> kJ	28.46	31.56	27.17	35.87	123.06	48.41	44.03	34.06	45.43	171.93
TQLOSS	10 <sup>6</sup> kJ	0.876	0.823	0.788	0.829	3.316	0.908	0.910	0.946	0.932	3.696
TQOVER	10 <sup>6</sup> kJ	0	0	0	0	0	0	0.108	3.828	0.892	4.828
E <sub>r</sub>	%	76.9	78.2	76.7	76.0	76.9	74.0	69.3	67.3	67.2	69.8
E <sub>e</sub>	%	67.2	68.0	67.3	66.9	67.3	65.4	62.5	61.3	61.2	62.7
E <sub>c</sub>	%	70.0	72.0	70.7	69.8	70.6	72.7	70.7	69.0	69.0	70.5
RC	%	61.42	67.39	49.72	64.12	60.37	78.76	52.40	39.70	52.51	53.79
CL	%	79.92	70.65	52.23	72.54	66.55	87.90	69.65	78.02	60.16	72.73
N		46	54	92	52	244	22	66	50	53	191

month, in Fig. 11(a,b), and the cooling load satisfied by the SSPRE is shown in Fig. 12(a,b). 66.6 percent of the total seasonal cooling load is satisfied by the SSPRE in Washington, D.C. and 72.7 percent in Phoenix, Arizona. Listed below the monthly bars in Fig. 11(a,b) are the monthly operating hours of the backup motor.

**3.3 Seasonal Performance.** The seasonal performance of the system in the "base-case" configuration is summarized in Tables 1 and 2. Several observations are noteworthy:

- As expected, when the electric energy used by the backup motor is included in the definition of the system COP, the fact that the efficiency of conversion of electric energy to cooling is higher than that of thermal energy to cooling make the COP increase with the fraction of the total energy supplied by this motor and may thus be misleading for evaluating solar-powered systems.

- The seasonal efficiency of the power cycle remains about double that of organic fluid cycles operating at similar solar collector temperatures.

- The COP of this base-case configuration is similar to or better than other solar cooling systems operating with the same collectors, chiller, and air-cooling (see [26, 27]).

- Although the needed collector investment in the SSPRE/cooling system is significantly lower than that for other solar cooling systems, the savings in electric energy consumption (and cost) in this "base-case" configuration are rather modest and reflect the economic weakness characteristic to existing solar cooling system in general.

**3.4 Improved System Configurations.** To examine the potential improvement of the system's performance, simulation runs were made for the month of August in Phoenix, Arizona, where the "base-case" configuration was altered by replacing the evacuated collectors with higher efficiency flat-plate ones, and the air-cooled power-cycle condenser by a water-cooled one.

Three cases with following configurations were studied:

- Case 1: The "base-case" evacuated-tube collector (see section 3.1) with a water-cooled power-cycle condenser.

**Table 2 Major results for the four-month simulation (May-August) of the base-case SSPRE/cooling system**

		Washington, DC	Phoenix, AZ
• Total Resource Energy used, (10 <sup>6</sup> kJ):			
Solar Energy	TYSOL	112.6	177.02
Fuel Energy	THFUEL	39.96	61.38
Electric Energy	E/n <sub>e</sub>	32.98/0.3	42.92/0.3
• Energy Fractions			
Solar Energy	ZSOL	42.9%	46.4%
Fuel Energy	ZFUEL	15.2%	16.1%
Electric Energy	ZE	41.9%	37.5%
Total		100%	100%
ZE:			
RC parasitic	ZAUX	3.9%	2.2%
Chiller parasitic	ZCHIL	18.7%	13.1%
Back-up motor	ZMOT	19.3%	22.2%
• % Contribution of Rankine Cycle			
To Total Cooling Load	%CL	66.5%	72.7%
To Total Power Demand	%RC	60.4%	53.8%
• Collector Efficiency			
	η <sub>coll</sub>	0.260	0.289
• Thermal Efficiency of Rankine Cycle			
	ZRANK	0.158	0.146
• Overall Rankine Cycle Efficiency			
	OZRANK	0.149	0.135
• Rankine Cycle Resource Efficiency			
	OZRANKR	0.142	0.131
• Chiller COP excluding Condenser Fan			
	COPNF	3.66	3.99
• Chiller COP with Condenser Fan			
	COP	2.65	3.13
• Overall System COP based on			
Total energy input	OCOPP	0.757	0.780
Resource energy input	OCOPR	0.627	0.575
Net energy conversion	OCOPS	0.877	0.967
Thermal energy input	OCOPT	0.649	0.796
• % Resource Energy Saving			
	ZSAV	22.1%	20.3%
• Electric Energy Saving (10 <sup>6</sup> kJ (kW-hr))			
	EES	28.76 (7989)	38.75 (10764)

- Case 2: Higher-efficiency flat plate collector, with the "base-case" air-cooled power-cycle condenser.

- Case 3: Higher-efficiency flat-plate collector with a water-cooled power-cycle condenser.

To simplify the analysis, and since only an upper bound was sought for the improvements, it was assumed that the

steam condensation temperature in the water-cooled condenser is the ambient dry-bulb temperature as read on an hourly basis from the meteorological data for Phoenix in August. For a similar reason, the incidence angle modifier of the higher-efficiency collector  $K_{\alpha\tau}$ , was assumed to be unity. The collector's efficiency equation was<sup>5</sup>

$$\eta_{\text{coll}} = 0.78 - 14.19 \left( \frac{T_i - T_a}{I} \right) \quad (27)$$

where the slope is in (kJ/hr m<sup>2</sup> °C). It is noteworthy that the peak efficiency of this collector is twice as high as that of the one described by equation (26), but its slope is about three times higher.

The major results of the runs are compared to those for the "basecase" in Table 3. By reducing the turbine back-pressure, water cooling (Case 1) increases the power cycle efficiency by 23.3 percent, which results also in an increase in the power cycle's contribution for satisfying the cooling load, and in significant increases in the resource energy saving ZSAV (56 percent), and electric energy saving EES (32.4 percent). The observed decreases in the coefficients of performance OCOPS and OCOPP are due to a decrease in the use of the electric backup motor, as explained in section 3.3 above.

In Case 2, the collector's average efficiency is 15.4 percent higher. The Rankine cycle's efficiency, however, remains essentially unchanged, because the top cycle temperature is kept the same (600°C). Since the thermal storage obtains more energy with these collectors, the Rankine cycle's contribution to driving the compressor increases, and so does the electric energy saving (+ 18.8 percent).

Combining both water-cooling and the higher-efficiency collectors in Case 3, results in an 85.5 percent increase in resource energy saving (ZSAV) due to the significantly higher contribution of the Rankine cycle, and a 56 percent increase in electric energy saving. The corresponding increase in fuel consumption for the superheater (THFUEL) is only 25.3 percent.

The results in Table 3 also demonstrate that the combined use of water cooling and higher-efficiency collectors provide performance which is better than that obtained by increasing the collector area by 50 percent. For example, the electric energy saving is larger by 15 percent, and the fuel consumption is reduced at the same time by 9 percent.

Further improvements in system performance can be obtained by using a chiller with a higher COP, by reducing the parasitic fan power, and by an optimal system control strategy. The latter is the subject of continuing research at the University of Pennsylvania. The impact of the two former methods can, however, be approximately assessed as follows:

1 Fan power use in the chiller's air-cooled condenser is significant and is calculated by the assumption that all fans are in operation whenever the chiller is on. Normally, however, the fan power would be lower, either by adjusting the fan power to the condensing need, or by better condenser or fan design. If all fan power was eliminated, the chiller performance would have increased by a factor of (COPNF/COP). Seasonally, this is 1.380 for Washington and 1.275 for Phoenix. If, as observed in many commercial installations, only half of the fans are in operation (on the average), the potential improvement factor is 1.19 for Washington and 1.14 for Phoenix, or 1.165 average.

2 In an analysis of a similarly sized chiller by Carrier [26], it was stated that the type of chiller used in the simulation had a seasonal COPNF of 4.7 (when averaged between New York and Phoenix). The chiller simulated here had an average COPNF of 3.8. Using the higher-performance chiller would have thus improved the COPNF by a factor of (4.7/3.8) = 1.24.

Table 3 Relative changes of performance due to the introduction of a higher-efficiency collector and water-cooling of the power-cycle condenser

Collector Area:	Base-Case Value, $A_{\text{coll},b}$			$1.5 A_{\text{coll},b}$
Parameter	Parameter Change, in %, for Case Number:			
	1	2	3	3
SRC	+ 25.9	+ 17.1	+ 46.5	+ 7.8
%CL	+ 20.2	+ 12.2	+ 33.5	+ 6.8
$\bar{\eta}_{\text{coll}}$	+ 1.6	+ 15.4	+ 18.6	+ 21.5
OZRANK	+ 23.3	+ 0	+ 23.3	+ 19.7
OCOPS	- 2.6	- 12.4	- 13.2	+ 10.6
OCOPP	+ 0.6	- 10.5	- 10.3	+ 19.7
ZSAV	+ 56.2	+ 19.6	+ 85.5	+ 38.6
THFUEL	+ 7.3	+ 17.9	+ 25.3	- 9.0
EES	+ 32.4	+ 18.8	+ 56.0	+ 15.0

For the month of August, the overall base-case system COP, including all losses, OCOPP, was 0.85 (as averaged between Phoenix and Washington). Consequently, by a reduction of chiller fan power, and by using a better chiller, the OCOPP may rise to (0.85)(1.165)(1.24) = 1.23.

The use of a water-cooled chiller will result in an additional improvement of ~ 10 percent, as shown above and in [23]. This may boost the OCOPP to 1.35.

#### 4 Conclusions

- A computer program was successfully developed for the transient simulation of hybrid solar-powered/fuel assisted power/cooling systems, based on comprehensive modeling of all of the system's components. The program allows easy change of component configuration to evaluate the system's performance sensitivity.

- Based on transient simulation, the seasonal thermal efficiency of the proposed Rankine system with the evacuated tube collector and air-cooled condenser (the base-case) is 15.8 percent in Washington, D.C. and 14.6 percent in Phoenix, Arizona. The thermal efficiency of the Rankine system with the water-cooled condenser (Case 2), is 17.9 percent for the month of August in Phoenix, for both types of collectors considered, as compared to 15.0 percent for the same month with the base-case configuration.

- The overall Rankine cycle seasonal efficiency based on total energy input, including the parasitic power, is 14.9 percent in Washington, D.C. and 13.5 percent in Phoenix for the basecase. By using the water-cooled condenser (Case 2), this value is elevated to 16.5 percent for August in Phoenix (as compared to 13.4 percent for the same month, base case). Again, it is the same for both types of collectors

- The overall system COP based on total net energy conversion, excluding parasitic energy, the seasonal (OCOPS), was found to be 0.88 in Washington, D.C. and 0.97 in Phoenix for the base case (air-cooled condenser, evacuated tube collectors, and a chiller with a seasonal COP ≈ 3.7).

- The overall system COP based on total energy input, OCOPP, in Phoenix is 0.816 for the basecase, 0.82 for Case 1, and 0.73 for Cases 2 and 3. Reduction of the chiller condenser's fan power to the practical value of 1/2 of that assumed in the simulation, the use of a higher performance chiller (COPNF = 4.7 as in [26]), and water cooling can increase the OCOPP to 1.35 (average value between Washington and Phoenix for August). Implementation of a water-cooled condenser and high-quality flat-plate collectors create a performance improvement which is superior to that created by adding 50 percent more of the evacuated collector area to the base case.

<sup>5</sup>Corresponding to an Ametek Co. flat-plate collector

## 5 Acknowledgment

The University of Pennsylvania graduate students, Stuart Bassler, Albert Lenng, Lee Ng, S. Subbiah, and Y. Tarkovski, and Professors H. Yeh, R. Kroon, and C. A. Meyer made important contributions to this work. The analysis of the chiller was based on information provided by the Trane Company under the supervision of Messrs. Dan Meeker and Monte Holman. The authors also wish to gratefully acknowledge the assistance and cooperation of Philadelphia Gear Corporation, The Trane Company, and United Engineers and Constructors, Inc., which were subcontractors to the University of Pennsylvania. This project was supported by the USDOE Solar Heating and Cooling Research and Development Branch.

## 6 References

- 1 Curran, H. M., "Assessment of Solar-Powered Cooling of Buildings," Hittman Associates, Final Report HIT-600, (NTIS:C00/2522-1), Apr. 1975.
- 2 Lior, N., "Solar Energy and the Steam Rankine Cycle for Driving and Assisting Heat Pumps in Heating and Cooling Modes," *Energy Conversion*, Vol. 16, 1977, pp. 111-123.
- 3 Merriam, R., "Solar Air Conditioning Study," NTIS Document No. AD/A-043-951, 1977.
- 4 Lior, N., Yeh, H., and Zinnes, I., "Solar Cooling Via Vapor Compression Cycles," *Proc. 1980 Annual Meeting, International Solar Energy Society, American Section*, Phoenix, Ariz., Vol. 3.1, 1980, pp. 210-214.
- 5 Lior, N., "Methods for Improving the Energy Performance of Heat Pumps," presented at the 9th Intersociety Energy Conversion Engineering Conf., San Francisco, Calif., Aug. 1974; also University of Pennsylvania MEAM Report No. 74-4, 1974.
- 6 Curran, H. M., and Miller, M., "Evaluation of Solar-Assisted Rankine Cycle Concept for the Cooling of Buildings," Paper No. 759203, *Proc. 10th IECEC*, 1975, pp. 1391-1398.
- 7 Koai, K., Lior, N., and Yeh, H., "Analysis of a Solar Powered/Fuel-Assisted Rankine Cycle for Cooling," pt. 1, *Proc. 1982 Annual Meeting, American Solar Energy Society*, Houston, Texas, 1982, pp. 573-578.
- 8 Kroon, R. P., Meyer, C. A., Lior, N., and Yeh, H., "Design of a 30 HP Solar Steam Powered Turbine," Topical Report DOE/ET/20110-3 (DE82007236), May 1980.
- 9 Martin, C. G., and Swenson, P. F., "Method for Converting Low Grade Heat Energy to Useful Mechanical Power," U.S. Patent No. 3,950,949 (for Energy Technology, Inc.), 1976.
- 10 DiPippo, R., Khalifa, H. E., Correia, R. J., and Kestin, J., "Fossil Superheating in Geothermal Steam Power Plants," *Proc. 13th IECEC*, Vol. 2, 1978, pp. 1095-1101.
- 11 Kestin, J., DiPippo, R., and Khalifa, H. E., "Hybrid Geothermal-Fossil Power Plants," *Mechanical Engineering*, Vol. 100, No. 12, 1978, pp. 28-35.
- 12 DiPippo, R., Kestin, J., Avelar, E. M., and Khalifa, H. E., "Compound Hybrid Geothermal-Fossil Power Plants: Thermodynamic Analyses and Site-Specific Applications," ASME Paper No. 80-Pet-83, 1980.
- 13 Klein, S. A., et al., "TRNSYS: A Transient System Simulation Program," Solar Energy Lab., University of Wisconsin, Madison, Version 10.1, June 1979.
- 14 Lior, N., Koai, K., and Yeh, H., "Analysis of the Solar-Powered/Fuel-Assisted Rankine Cycle Cooling System," Report SAN/20110-5, submitted to the USDOE, Dec. 1981.
- 15 Kern, D. Q., and Kraus, A. D., *Extended Surface Heat Transfer*, McGraw-Hill, New York, 1972.
- 16 Kern, D. Q., *Process Heat Transfer*, McGraw-Hill, New York, 1950.
- 17 Webb, R. L., "Air-Side Heat Transfer in Finned Tube Heat Exchangers," *Heat Transfer Engineering*, Vol. 1, No. 3, 1980, pp. 33-49.
- 18 Rohsenow, W. M., and Hartnett, J., eds., *Handbook of Heat Transfer*, McGraw-Hill, New York, 1973, pp. 12-19.
- 19 Goldstern, W., *Steam Storage Accumulators*, Pergamon Press, London, 1970.
- 20 Talaat, M. E., "A Pressurized-Liquid Concept for Solar-Thermal Energy Storage," *AIChE J. Energy*, Vol. 2, 3, 1978, pp. 136-141.
- 21 Miyatake, O., Murakomi, K., Kawata, Y., and Fujii, T., "Fundamental Experiments with Flash Evaporation," *Heat Transfer, Japanese Research*, Vol. 2, 4, 1973, pp. 89-100.
- 22 Swamee, P. K., and Jain, A. K., "Explicit Equations for Pipe-Flow Problems," *J. of the Hydraulics Div., Proc. ASCE*, Vol. 102, 5, 1976, pp. 657-667.
- 23 The Trane Company, La Crosse, WS, "Chiller Performance Data for Model I-CAUA-C25-B, 1-CCOA-C255-C," SSPRE Project subcontractor correspondence, Sept. 1979.
- 24 Leboeuf, C., "Standard Assumptions and Methods for Solar Heating and Cooling Systems Analysis," SERI/TR-351-402, Solar Energy Research Institute, Jan. 1980.
- 25 Wyle Laboratories, "Indoor Test for Thermal Performance of the Sunmaster Evacuated Tube (Liquid) Solar Collector," DOE/NASA Contractor Report CR-161306, Sept. 1979.
- 26 English, R. A., "Development of a High-Temperature Solar Powered Water Chiller," Report SAN-1590-1, U.S. Department of Energy, June 1978.
- 27 United Technologies Research Center, "Design, Development and Testing of a Solar-Powered Multi-Family Residential Prototype Turbocompressor Heat Pump," Final Technical Report No. R79-953050-1 to U.S. Department of Energy, Sept. 1979.